sustainability

MDPI

Article

A Precise Energy Consumption Model for Computer Numerical Control Machines: A Hybrid Approach

Saime Taphasanoğlu [1], Muhammet Raşit Cesur [2,*] and Elif Cesur [2]

[1] Industrial Engineering Department, Istanbul Rumeli University, 34570 Istanbul, Turkey
[2] Industrial Engineering Department, Istanbul Medeniyet University, 34700 Istanbul, Turkey
* Correspondence: rasit.cesur@medeniyet.edu.tr; Tel.: +90-5443932918

Abstract: In today's world, energy efficiency is becoming increasingly crucial, due to its impact on sustainability in production. Designing systems that consume less energy and manage resources efficiently is essential. Variations in operating speed can affect processing time, energy consumption, idle times of subsequent machines, work delays, and missed deadlines. While most studies focus on prediction parameters like cut depth and cut area to estimate the energy consumption or processing time, our approach emphasizes variations in G-code motion parameters. To enhance both precision and the adaptability of the model to all Computer Numerical Control (CNC) machines in no-load condition, we propose an intelligent hybrid model that combines physical and data-driven approaches. The first approach employs curve fitting based on the physical model, while the second utilizes deep neural network (DNN) models optimized through hyperparameter tuning. The DNN topologies we evaluated exhibit high performance, with prediction errors of less than 1% for all models. Our approach provides a more precise and comprehensive understanding of energy consumption patterns in manufacturing processes, enabling manufacturers to make informed decisions about energy utilization, cost reduction, and sustainability. Our study aims to advance the field of energy efficiency in manufacturing and contribute to a more sustainable future.

Keywords: energy efficiency; CNC; DNN; Industry 4.0

check for updates

Citation: Taphasanoğlu, S.; Cesur, M.R.; Cesur, E. A Precise Energy Consumption Model for Computer Numerical Control Machines: A Hybrid Approach. *Sustainability* **2024**, *16*, 10659. https://doi.org/10.3390/su162310659

Academic Editor: Maxim A. Dulebenets

Received: 19 October 2024
Revised: 17 November 2024
Accepted: 30 November 2024
Published: 5 December 2024

1. Introduction

Sustainable production has emerged as a pivotal component in alignment with the European Commission's green production objectives for Industry 5.0 [1]. It has also been a critical topic in the broader sustainability discourse over the past few decades. To enhance sustainability in production, reduce carbon emissions, and optimize resource utilization, the scientific literature is now focusing on energy efficiency-oriented research [2]. These studies delve into allocating alternative robots or CNC machines in ways that minimize energy consumption, and determining the optimal machine speed to curtail total energy usage [3–6]. Determining the optimal machine speed offers a more effective solution, as it ensures the efficient operation of all production resources. However, solely evaluating energy consumption in such optimization studies overlooks numerous parameters influencing the production system, potentially hindering the attainment of applicable results. For instance, slowing down all CNC machines and robots to minimize energy consumption can lead to production delays. Thus, reducing the energy consumption of automation systems hinges on factors beyond operating parameters, such as production planning, material requirement planning, facility layout, and product design. Although most studies optimize the energy consumption of automation systems individually, global optimization of the operating parameters for these interconnected systems would significantly strengthen energy efficiency.

Within energy efficiency studies, parameters like processing time, machine idle time, energy consumption during processing, and energy consumption during idle periods are thoroughly assessed [3–8]. However, these optimization studies typically evaluate processing time and energy consumption at discrete speed levels (e.g., slow, normal, or maximum) or assume a constant speed when considering job dispatching across alternative machines [9]. In practice, machine speeds can be dynamically adjusted, leading to variations in operation time. Therefore, an energy consumption optimization model should account for variations in operation time based on machine speed, the corresponding changes in energy consumption, and the total energy usage over the operation period for each machine alternative individually. In addressing this gap, dynamic models are a rarity in scheduling studies [10]. Our goal is to propose a predictive model for processing time and energy consumption under no-load conditions, based on CNC machining parameters, which can be integrated into iterative optimization models for energy-efficient scheduling. The model is designed to predict motion within a 0-to-3-meter range and to simulate only linear and arc/circular movements, a range commonly applied to most CNC routers. While it is theoretically expected to function beyond this range, performance for displacements exceeding 3 m has not been validated. Additionally, the model does not account for spindle energy consumption or material hardness, as these factors are not critical to optimizing machine configuration. Our key contribution lies in calculating total processing time and energy consumption by analyzing each individual G-code line, rather than relying on parameters such as cutting area, depth, or material hardness, as is common in most studies. This approach combines machining parameter optimization with scheduling tasks to achieve a comprehensive, global optimization. It represents a novel contribution to sustainable and smart manufacturing, addressing a gap in the current scientific literature.

1.1. Literature Review

Over the past few decades, sustainability has been a significant topic, and researchers have conducted numerous energy efficiency-focused studies to enhance sustainability in production. Achieving sustainability in production systems from an energy perspective involves different aspects. One key aspect involves developing energy-efficient production technology, necessitating additional investment in existing production systems [11–14]. Another crucial aspect is the implementation of renewable energy production systems, such as wind turbines and solar cells [15–18], as well as hybrid power generation systems that combine solar and wind power. These hybrid systems maximize energy efficiency by taking advantage of the complementary nature of solar and wind resources, ensuring a more stable energy supply. However, while they offer advantages like enhanced reliability and environmental benefits, they also present challenges, such as higher initial costs and complex maintenance requirements [19–21].

While most energy-driven scheduling studies focus solely on optimizing specific machine speeds, some highlight the importance of optimizing machining parameters such as cutting speed, feed rate, and depth of cut, to enhance energy efficiency [22]. Comparative analyses between dry-cutting and wet-cutting CNC hobbling machines reveal that dry cutting offers superior efficiency, despite higher energy consumption [23]. This highlights the trade-off between operational efficiency and energy consumption in the context of scheduling. Practical measurements and experimental results underscore the fact that even small adjustments in machining processes can lead to substantial energy savings [24], without significantly compromising operational efficiency. Consequently, continuous innovation and optimization in CNC machining [25] play a crucial role in advancing sustainability efforts.

To improve energy efficiency and optimize resource utilization, scholars have undertaken research aimed at examining the distribution of substitute machines or determining the ideal machine speed to minimize overall energy consumption [3–6]. The impact of altering machine speeds on production schedules is an infrequently addressed subject in the scientific literature [10]. Researchers in the scientific literature have utilized the interpolation method to model this particular effect [26,27]. Our study differs from the mentioned studies in that. However, it is well known that the relationship between the feed rate of motion and time is not necessarily linear. In this context, it has been found that changes in feed rate caused by trajectory optimization have an impact on cycle time [26,28]. So far, artificial neural network-, curve fitting-, Gaussian process- and extreme learning machine-based approaches have been developed to predict these changes. The solutions presented in References [29–33] are summarized in Table 1, along with their mean absolute percentage error (MAPE) and R^2 values, which represent the square of Pearson's correlation coefficient between the actual and predicted data.

Table 1. Performance of the best topologies for linear motion.

Method	Prediction Context	MAPE (%)	R^2	Citation
Extreme Learning Machine	Energy Consumption	4.37	0.9928	[29]
Artificial Neural Network	Energy Consumption	0.18	0.9999	[30]
Curve Fitting	Energy Consumption	0.43	0.9998	[30]
Artificial Neural Network	Cycle Time	2.26	0.9992	[31]
Curve Fitting	Energy Consumption	5.09	0.998	[32]
Gaussian Process Regressor	Energy Consumption	3.4	0.9952	[33]

1.2. Research Gap and Motivation

In the scientific literature, energy optimization studies primarily focus on trajectory optimization, machining parameter optimization, and job allocation to alternative machines. For machining parameter optimization, key factors such as cutting speed, feed rate, depth of cut, cutting area, and material hardness are often addressed. These parameters are commonly used to predict the total energy consumption of the machining process. This may be due to the fact that CNC boards provide data on displacement and energy consumption over specific time periods (typically spanning a few lines of G-code), making it difficult to isolate energy consumption or displacement duration for smaller, individual motions. Additionally, when larger displacements occur, CNC boards may provide multiple lines of sensor data for a single line of G-code. This technical limitation may lead to the correlation of process volume and material hardness with total energy consumption and machining duration.

We aim to propose a model that can predict the energy consumption for each individual line of G-code sent to a CNC machine. This approach is expected to significantly enhance the precision of machining parameter optimization. Furthermore, by predicting machining time, our model will enable the optimization of machining parameters in conjunction with manufacturing planning and control functions. To achieve this, we eliminate parameters that are not directly related to machining, and propose a model to predict the machine's energy consumption under no-load conditions. Our study addresses several critical gaps in the existing scientific literature within this domain.

1. Researchers in the scientific literature have employed interpolation methods to model this particular effect [26,27]. However, these methods need not be limited to linear interpolation.
2. Although different artificial neural network techniques were used to develop these solutions, they frequently employed a single hidden-layer topology [29,31]. However, small displacements cannot be correlated with machining parameters in the same way as larger displacements. Therefore, a deep learning (DL) model is necessary.
3. Energy optimization studies concentrate on adjusting machining speeds and consider specific speeds for machining [10]. Our model can operate at any machine speed, as it predicts energy consumption based on machine speed, which is treated as a continuous variable.
4. We proposed a comprehensive model to contribute to the scientific literature and support practitioners by evaluating each line of G-code individually. This approach allows for the adjustment of the feed rate parameter in the G-code to optimize energy

prediction while adhering to machining time constraints. The capability of our model facilitates the integration of scheduling and manufacturing engineering functions.

1.3. Contribution and Paper Organization

Our methodology, presented in Figure 1, aims to develop an energy consumption model based on physical equations that factor in processing time and unit energy requirements relative to the feed rate. This enables the design of an AI model capable of inferring the working dynamics of CNC machines by evaluating the G-code sent to them. In doing so, the model contributes to the scientific literature by introducing a G-code-driven prediction approach and a hybrid model that combines features derived from both physical equation calculations and data collected from CNC machines. Our study presents two key innovations. First, it incorporates calculations from the physical model as inputs to the AI model. Second, it calculates energy consumption and processing time for each individual line of G-code, enabling the integration of manufacturing engineering and scheduling functions.

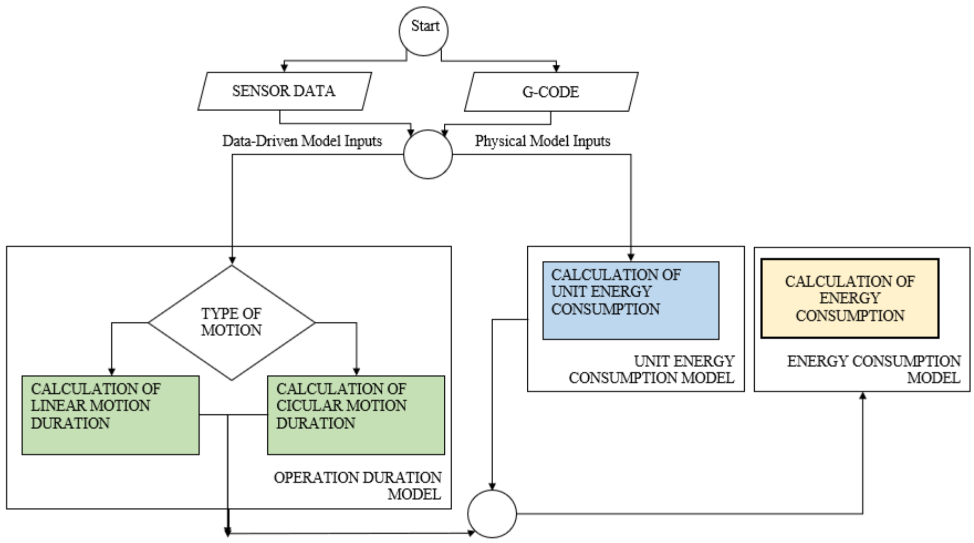

Figure 1. Structure of proposed model.

We explored both curve fitting and deep neural network (DNN) methods to identify the most suitable methods. Firstly, we created two distinct models for estimating the duration of linear motion and arc/circle motion, both grounded in the same physical principles with curve fitting. At the second step, we created a linear regression model to predict unit energy consumption at any machine feed rate. Finally, we calculated total energy consumption by multiplying the processing time by unit energy consumption, based on physical equations. Additionally, we utilized a deep neural network (DNN) model to estimate both operation duration and energy consumption, offering a performance improvement over curve fitting and surpassing the capabilities of the proposed physical model. To further improve the network topology, we performed hyperparameter optimization using iterated local search as a meta-heuristic method. As a result, we developed a model that is both precise and adaptable for predicting processing time and energy consumption. The DNN model, based on physical relationships, demonstrates superior performance in predicting operation duration and energy consumption. This hybrid model represents a significant contribution of our study to the scientific literature.

The next section provides the research background on energy consumption models and methods, establishing the foundation for our study. Following this, we propose both physical and data-driven models, detailing their development and theoretical basis. The next chapter reviews key deep learning (DL) techniques commonly used in industry. DL models excel in supervised tasks with large datasets, but still face challenges with complex reasoning. A DNN includes various layers for input processing, feature extraction, and regularization, using techniques like convolution and recurrent layers to enhance performance. Consequently, we present a numerical analysis and explore the application of DNN methods to our models. This is followed by a section discussing the results of our analysis and their implications. Finally, the paper concludes with a summary of our findings and suggestions for future research.

2. Materials and Methods

To ensure our model is applicable to various machines and robots, we developed a hybrid model that integrates both physical and data-driven approaches, utilizing data collected from CNC machines. Our methodology involved constructing models for both linear and arc/circle motions. By employing interpolation techniques on the experimental dataset, we derived linear equations, polynomial equations, and Fourier series. We explored curve fitting and DNN methods to identify the most suitable models for our purposes. Our preference for DNNs stems from their ability to differentiate between minor motions, which do not reach the feed rate specified in the G-code, and standard motions performed at the specified machine speed. This approach aims to develop a more precise model for accurately predicting processing time and energy consumption across various displacement and feed rate combinations. As a result, we created two distinct models for estimating the duration and energy consumption of both linear and arc/circular motions, all based on the same underlying physical principles. This approach improves the precision of our system, while transfer learning enables the DNN to adapt across different machines. The DNN model serves as a foundational tool, offering both precision and adaptability. It represents a significant contribution to the scientific literature by demonstrating high accuracy and versatility across a wide range of applications.

2.1. The Physical Model of Operation Duration and Energy Consumption

The operational efficiency of a machine hinges on two fundamental factors: the time allocated to its physical motions and the duration of other processes that induce waiting periods. As such, the total operational time can be ascertained by summing the projected travel time of the tool head and the scheduled waiting intervals described in the G-Code. To predict the displacement duration (T), we use data concerning the tool's displacement (m) and its associated feed rate as velocity (v), which are also gathered from the G-Code. This relationship is expressed in Equation (1).

$$T = \frac{m}{v} \tag{1}$$

As the stepper motor operates over the specified distance at the predetermined speed, Figure 2 illustrates the cumulative durations of acceleration, constant speed displacement, and deceleration, which collectively constitute the total operational time of the stepper motor.

The total displacement, as presented in Equation (2), is the sum of the displacements during acceleration (m_a), deceleration (m_d), and constant motion (m_c).

$$m = m_c + m_a + m_d \tag{2}$$

Consequently, the execution time of each command must be calculated on an individualized basis for each machine, as the execution duration of these commands is contingent upon the mechanical configuration of the machine and the control algorithm integrated into the CNC board. To ascertain the duration of the displacement, we use the f function in Equation (3) to represent a basic physical model.

$$f_{mv} = m_c + 2m_a + 2m_{dv} \tag{3}$$

The total duration of acceleration and deceleration motion, (T_{ad}), is expressed by m_a, m_d and v, as given in Equation (4).

$$T_{ad} = \frac{2(m_a + m_d)}{v} \quad (4)$$

Because m_a and m_d are not known, Equation (5) is used for finding total acceleration and deceleration time. We investigated two different displacements: one is a specific displacement, and the other is twice the size of the first displacement. The difference between twice the duration of the first displacement and the duration of the second displacement will help us determine the half of total acceleration and deceleration time. as given in Equation (6).

$$2f\left(\frac{m}{v}\right) - f\left(\frac{2m}{v}\right) = 2\left(\frac{m_c + 2m_a + 2m_d}{v}\right) - \left(\frac{m + m_c + 2m_a + 2m_d}{v}\right) \quad (5)$$

$$\frac{m_c + 2m_a + 2m_d - m}{v} = \frac{m_a + m_d}{v} = \frac{T_{ad}}{2} \quad (6)$$

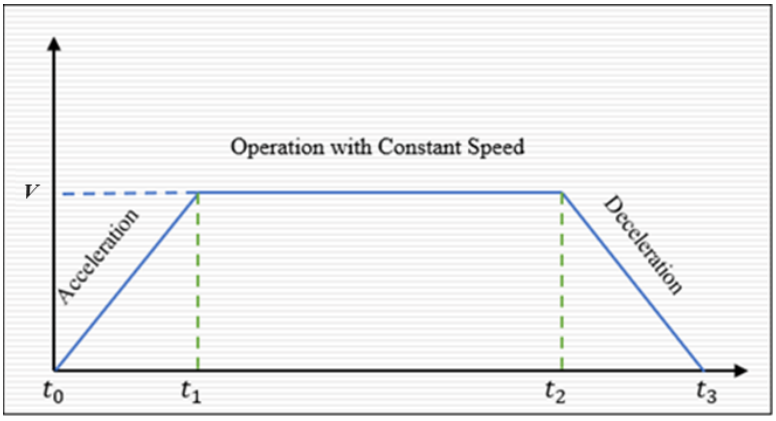

Figure 2. Velocity–time graph of motion.

First, the models will infer the correlation between motion parameters (linear, arc/circle) in G-Code and the duration of processing. The motion parameters include the amount of motion for axes (X, Y, Z, A, B, C), and the feed rate (F) of the motors. The maximum amount of linear motion resulting from the (X), (Y) and (Z) parameters, as well as the value of the F parameter, directly affects the duration of the motion. There are two fundamental types of circular movements: circular and elliptical. In G-code, the radius for circular movements is represented by "R". For elliptical arc movements, the offset parameters "T" and "J" indicate how to draw the ellipse. The duration of the motion for an arc or circle depends on the amount of circular motion to be executed, which, in turn, depends on the parameters X, Y, R or X, Y, I and J, as well as the value of the F parameter.

$$m = \max(x \in \{X,\ Y,\ Z,\ A,\ B,\ C\}) \quad (7)$$

The variables, beginning with point $(X_b,\ Y_b)$, target point $(X_t,\ Y_t)$ with the radius (r) or offset $(I,\ J)$ are used to calculate the length of arc/circle motion. The radius is not given directly; it can be calculated as given in Equation (8).

$$r = \sqrt{I^2 + J^2} \quad (8)$$

The total angle (θ) of the arc/circle displacement is given in Equation (9). The total displacement (M) regarding the angle and radius is given in Equation (10).

$$\theta = arcsin\left(\frac{\sqrt{(X_t - X_b)^2 + (Y_t - Y_b)^2}}{2r}\right) \tag{9}$$

$$M = 2\pi r \frac{\theta}{360} \tag{10}$$

The total consumed power ($P(v)$) during the processing time, defined by the function f, is the sum of the total displacement power ($P_d(v)$), the total power consumption of the machining head $(P_m(v))$, and the total idle power (P_i) at a specific feed rate v over the period T, as shown in Equation (11), following the methodology in [5,8].

$$P(v) = \int_{t=0}^{T} P_d(v)dt + \int_{t=0}^{T} P_m(v)dt + \int_{t=0}^{T} P_i dt = \int_{t=0}^{T} (P_d(v) + P_d(v) + P_i)dt \tag{11}$$

By generalizing the function (f) representing the proposed physical model in the study, we aim to make it applicable to various machines or robots. To achieve our goal, we developed the proposed a model based on the physical model provided in Equations (1)–(11) and a data-driven model using data collected from CNC machines. As a result, our model is both precise and adaptable to various machines. This hybrid model represents a significant contribution of this study to the scientific literature.

To represent the physical model in the data-driven model, we implemented the "m/v" parameter as an input for the developed models, as the processing time is equal to "$f(m/v)$". In the next step, we constructed models representing the "f" function for both linear and arc/circle motions. We investigated both curve fitting and DNN methods to find the most suitable models. Given this fact, two different models for estimating the duration of linear motion and arc/circular motion were created, based on the same physical model. The models show the relationship between m/v chosen as input (I) and the duration of displacement (T) as an output (O), estimated as processing time. This relationship could be represented in terms of the coefficients (A) of the function derived by curve fitting, as shown in Equation (12).

$$A = \left(I^T I\right)^{-1} I^T O \tag{12}$$

We obtained linear equations, polynomial equations, and Fourier series through interpolation using the experimental dataset. Additionally, we utilized the DNN to achieve superior performance, compared to the proposed model.

2.2. Deep Neural Networks

DL encompasses a variety of goals, although some approaches are still in the process of maturing. In our study, we focus on techniques that have already gained widespread adoption in industry. Modern DL excels in supervised learning scenarios, where increasing the number of layers and units within neural networks enables them to handle more complex functions. When dealing with tasks that involve rapid associations between inputs and outputs, DL performs admirably, especially when provided with large models and extensive labeled datasets. However, it still faces challenges when tackling tasks that demand deeper reasoning or complex thought processes.

At its core, DL draws inspiration from connectionism, in which nodes of the network can collectively exhibit intelligent behavior. The critical factor here is the network's size. Over the past few decades, neural networks have grown significantly in scale, contributing to their improved accuracy and ability to solve complex problems. Despite this growth, artificial neural networks remain comparable in size to the nervous systems of insects. Consequently, DL heavily relies on high-performance hardware and software to support these expansive networks.

A DNN, a fundamental technology in deep learning (DL), consists of several layers. These include an input layer, preprocessing layers such as Mel spectrogram, category encoding, discretization, hashed crossing, hashing, and normalization. Feature extraction layers include convolution, pooling, gated recurrent units (GRUs), dot, average, multiply, masking, and multihead attention. Regularization layers like dropout, L1, and L2 help prevent overfitting. Additionally, network-specific layers such as LSTM, RNN, dense, and flatten are used to refine the model's architecture. The DNN utilizes various activation functions, including ReLU, leaky ReLU, PReLU, swish, GELU, ELU, maxout, and multi-head attention. These components, presented in Figure 3, are integral to the topology of a DNN.

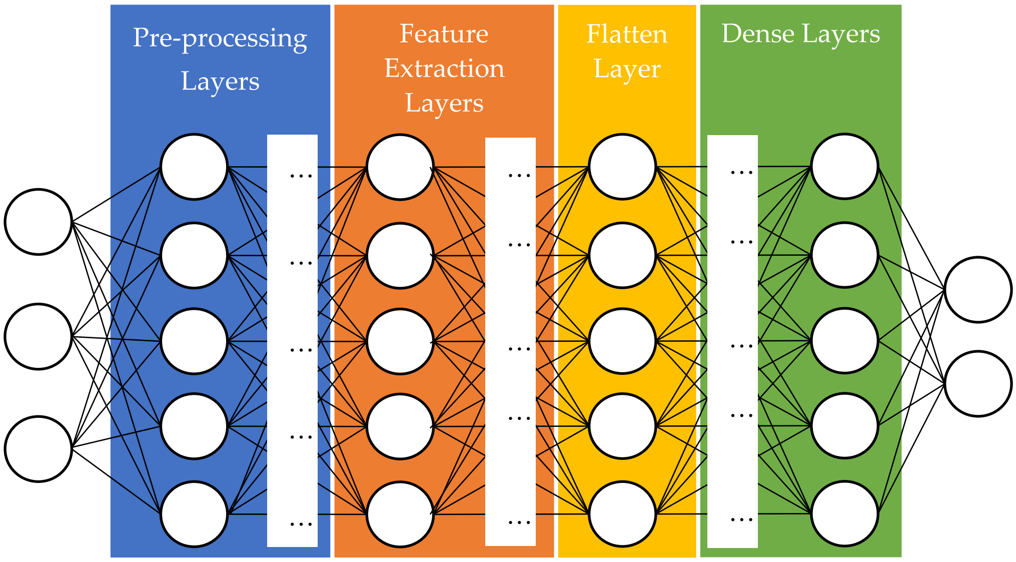

Figure 3. DNN Topology.

2.3. Performance Metrics

We compared models from the perspective of two performance metrics in this study. The first metric is mean absolute percentage error (MAPE), which provide the average error rate in the predicted data. This metric, also, present an accuracy which equals "1- MAPE". MAPE, presented in Equation (13), is the mean of the absolute percentage errors, calculated by taking the average of the absolute difference between the predicted (P) and actual (A) values, divided by the actual value. n is the number of the predicted data.

$$MAPE = \frac{\sum_{i=1}^{n} \left| \frac{A_i - P_i}{A_i} \right|}{n} \tag{13}$$

The other metric is R^2, presented in Equation (14), which is the square of Pearson's correlation coefficient. R^2 presents the power of the modelling trend or variance in the dataset.

$$R^2 = correlation(A,\ P)^2 \tag{14}$$

3. Case Study: Operation Duration and Energy Consumption

While investigating a precise method for predicting energy consumption, we conducted an experimental model development study using a CNC board equipped with NEMA 17 stepper motors, a current measurement sensor, and a microcontroller for sensor control and time measurement. Using this hardware, we first generated a dataset to predict processing time and energy consumption for both curve fitting and deep-learning model development. This approach enabled us to examine how well mathematical equations capture the correlation between physical parameters and operational outcomes, while also assessing how artificial intelligence can enhance these predictions beyond traditional mathematical models. Finally, we compared both models and analyzed the impact of input parameters to identify alternatives in terms of cost and precision.

The novel contribution of this study is the development of a predictive model for both operation duration and energy consumption, using direct G-Code parameters. Unlike most studies, which require parameters like cut depth and cut area to be calculated from G-Code, our approach leverages these parameters directly. Our goal is to develop models that capture the characteristics of CNC machines and robots by directly utilizing their operational parameters. To uncover the inherent properties of these machines, we collect data under no-load conditions. This allows us to create a DNN model that can serve as a pretrained model for predicting operational outcomes across different machines and materials.

Two data sets were created for the physical model and used to develop the linear and arc/circle motion models. These models were tested using a four-axis CNC board with NEMA 17 stepper motors. The CNC board is installed as software, which was developed as part of the GRBL project [34]. To measure the motion duration in real-time, an INA 219 current sensor with a frequency of 500 kHz and an Atmega-328P microcontroller, controlled by a 16 MHz crystal, were used. The time was recorded using the microcontroller's internal 8 MHz clocks. Real-time monitoring is crucial for correlating each action with individual lines of G-Code, as CNC boards do not report actions on a per-command basis. Instead, they provide aggregated data, such as total power consumption and displacement over a specific time interval, typically one second. This makes it difficult to track minor actions or distinguish between consecutive actions that may begin and end within the same second.

The dataset contains information about the feed rate, the amount of displacement, and the duration. We consider the ratio of displacement to velocity, referred to as the feed rate, as the input for all developed models. Feed rates and the number of displacements were organized for all possible combinations of the parameters listed in Table 2.

Table 2. Performance of the Long Short-Term Memory Model.

Linear Motion		Arc/Circle Motion	
Feed Rate (mm/min)	**Motion Amount (cm)**	**Feed Rate (mm/min)**	**Motion Amount (cm)**
125, 250, 500, 750, 1000	15, 25, 35, 50, 65, 75, 85, 100, 115, 125, 135, 150, 165, 175, 185, 200, 215, 225, 235, 250, 285, 300	125, 250, 300, 500, 600, 700	10π, 25π, 50π, 75π, 100π, 125π, 150π

In the case of the DNN, both the amount of displacement and velocity are used as additional inputs. The duration and power consumption per second serve as outputs of the proposed models. Finally, we calculate the total power consumption by multiplying the duration and power consumption per second.

4. Results and Discussion

4.1. Curve Fitting

In the model development phase, we began by investigating the correlation between the physical model parameter "m/v" and operation time, as well as power consumption. The same inputs and outputs were used for both linear and arc/circle motion models. When developing motion models, our initial approach involved exploring the possibility of finding a mathematical correlation through curve fitting. Curve fitting models have only a single input and a single output. Consequently, we developed time prediction and power consumption models separately.

To predict linear motion duration, we employed the linear function $t(x)$ described in Equations (15) and (16). This method enabled us to calculate displacement duration with an 8.36% MAPE and an R^2 value of 0.9985, indicating perfect model fit. Similarly, the linear model for estimating energy consumption, $p(x)$, presented in Equation (16), achieved a

MAPE of 18.83% with an R^2 value of 0.9951. Figure 4a illustrates the R^2 graph of the $t(x)$, while Figure 4b displays the R^2 graph of the $e(x)$ functions.

$$x = \frac{m}{v} \Rightarrow t(x) = 1964.24 + 93182.1x \quad (15)$$

$$e(x) = 33.4621 + 657.753x \quad (16)$$

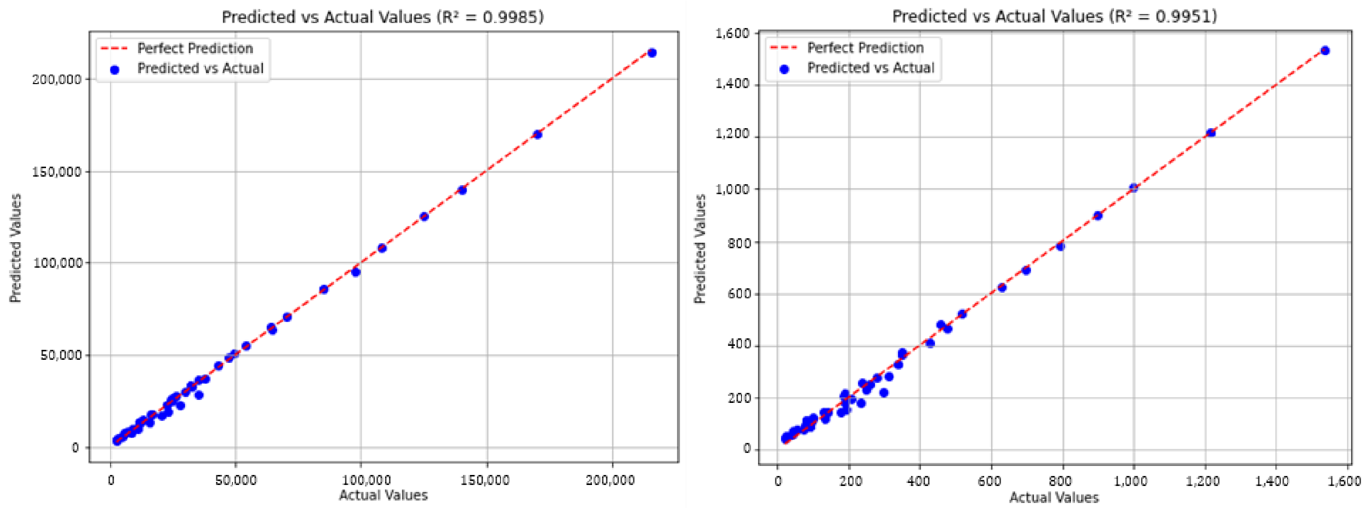

(**a**) (**b**)

Figure 4. (**a**) R^2 graph of operation-duration prediction model. (**b**) R^2 graph of energy-consumption prediction model.

The displacement time was estimated using a 9th-order polynomial, as described in Equations (16) and (17), where the lowest average error rates were observed. The MAPE for this polynomial model was 6.99% for operation duration and 9.77% for energy consumption. The R^2 value for the operation-duration prediction model, presented in Figure 5a, is 0.9977, while the R^2 value for the energy-consumption prediction model, displayed in Figure 5b, is 0.9951. The non-linear model outperforms the linear model, achieving error rates between 5% and 10% for both operation-duration and energy-consumption predictions. This indicates that the problem is more complex and requires more advanced methods beyond polynomial curve fitting for optimal results.

$$\begin{aligned} t(x) = \; & 696.257 + 96447.6x + 206252x^2 - 1.38105E6x^3 + 3.60814E6x^4 \\ & -4.92978E6x^5 + 3.84871E6x^6 - 1.72893E6x^7 + 415875x^8 \\ & -41479.3x^9 \end{aligned} \quad (17)$$

$$\begin{aligned} e(x) = \; & 6.78124 + 669.865x + 3198.15x^2 - 18073.7x^3 + 42715.4x^4 \\ & -54313.6x^5 + 40101.9x^6 - 17222.6x^7 + 3992.75x^8 \\ & -386.284x^9 \end{aligned} \quad (18)$$

The Fourier Series, as described in Equations (19) and (20), optimized with eight coefficients. The operation-duration prediction model achieved a MAPE of 7.34% and the energy-consumption prediction model one of 10.73%. The R^2 value for the operation duration model is, as displayed in Figure 6a, 0.9968, while the energy consumption model, illustrated in Figure 6b, has an R^2 of 0.9943, demonstrating strong adaptation to variations. However, the accuracy is insufficient for practical application.

$$\begin{aligned} t(x) = \; & -172873 + 281602(sin(x) + cos(x)) - 184939(sin(2x) + cos(2x)) \\ & +123112(sin(3x) + cos(3x)) - 76535.2(sin(4x) + cos(4x)) \\ & +43610.2(sin(5x) + cos(5x)) - 20063.8(sin(6x) + cos(6x)) \\ & +7541.2(sin(7x) + cos(7x)) - 1140.32(sin(8x) + cos(8x)) \end{aligned} \tag{19}$$

$$\begin{aligned} e(x) = \; & -1375.72 + 2156.36(sin(x) + cos(x)) - 1375.76(sin(2x) + cos(2x)) \\ & +935.227(sin(3x) + cos(3x)) - 573.871(sin(4x) + cos(4x)) \\ & +333.632(sin(5x) + cos(5x)) - 151.763(sin(6x) + cos(6x)) \\ & +60.8621(sin(7x) + cos(7x)) - -10.432(sin(8x) + cos(8x)) \end{aligned} \tag{20}$$

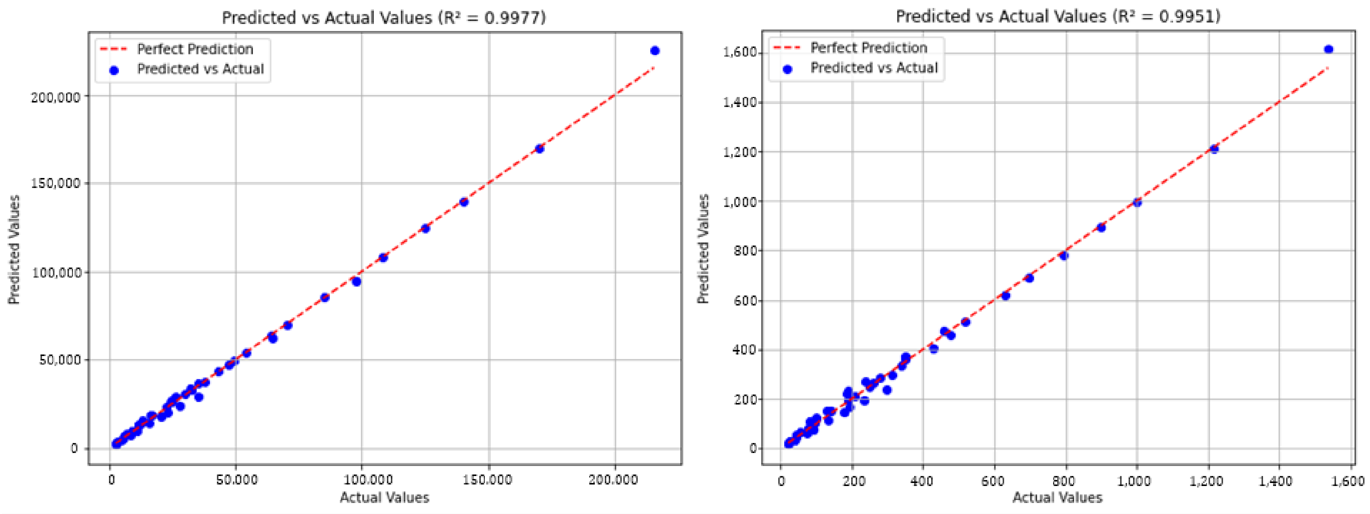

(**a**) (**b**)

Figure 5. (**a**) R^2 graph of operation-duration prediction model. (**b**) R^2 graph of energy-consumption prediction model.

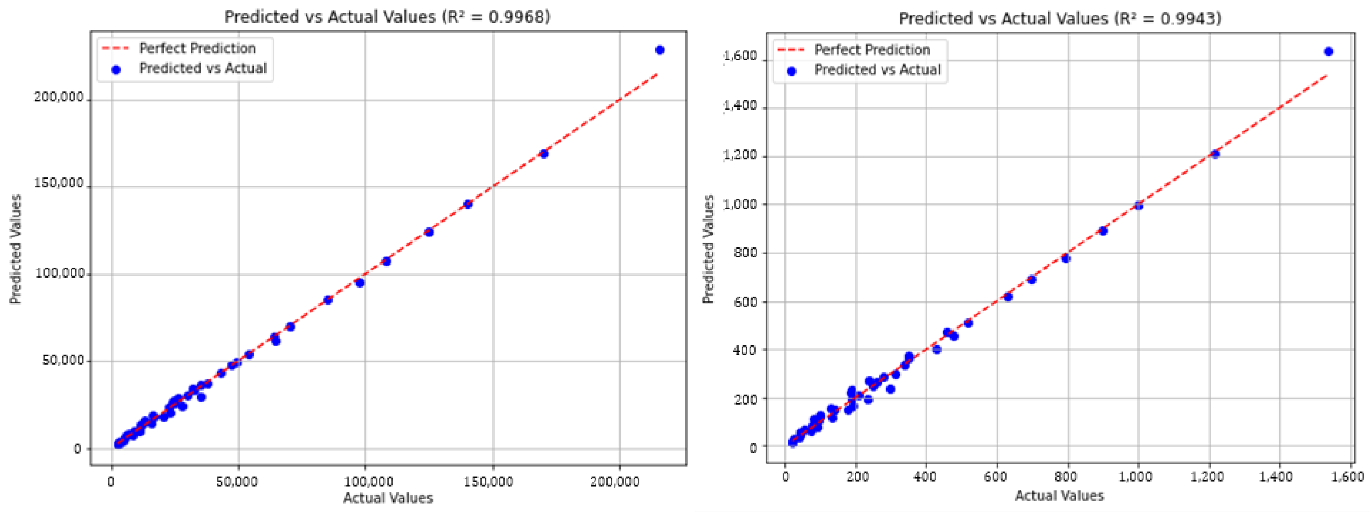

(**a**) (**b**)

Figure 6. (**a**) R^2 graph of operation-duration prediction model. (**b**) R^2 graph of energy-consumption prediction model.

Arc/circular motion differs from linear motion, in that its magnitude is π times that of the G-Code parameters. To account for these differences, we developed separate prediction models for arc/circular motion and linear motion. For the arc/circular model, we applied linear regression, as described in Equations (21) and (22). This yielded a MAPE of 6.27% for the operation-duration prediction model and 28.83% for the energy-consumption prediction model. The R^2 value for the operation-duration prediction model, shown in Figure 7a, is 0.9973, while the R^2 value for the energy-consumption prediction model, shown in Figure 7b, is 0.8733.

$$t(x) = 2813.82 + 185590x \tag{21}$$

$$e(x) = 72.1684 + 614.307x \tag{22}$$

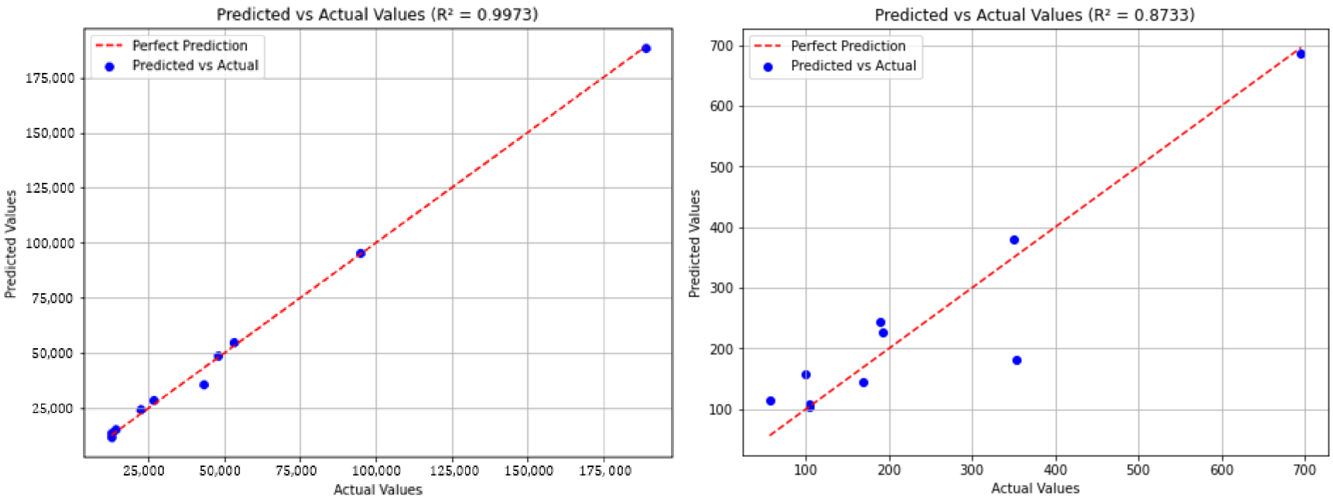

(**a**) (**b**)

Figure 7. (**a**) R^2 graph of operation-duration prediction model. (**b**) R^2 graph of energy-consumption prediction model.

The best-performing nonlinear models are the second-order polynomial functions described in Equations (23) and (24). The MAPE for the operation-duration prediction model in Equation (23) is 6.28%, while the MAPE for the energy-consumption prediction model in Equation (24) is 30.08%. The R^2 value for the operation-duration prediction model, shown in Figure 8a, is 0.9973, and the R^2 value for the energy-consumption prediction model, shown in Figure 8b, is 0.8678.

$$t(x) = 2947.2 + 184575x + 985.172x^2 \tag{23}$$

$$e(x) = 55.493 + 741.251x - 123.167x^2 \tag{24}$$

The Fourier series models, detailed in Equations (25) and (26), are constructed using two coefficients. The MAPE for the operation-duration prediction model in Equation (25) is 8.22%, while the MAPE for the energy-consumption prediction model in Equation (26) is 29.02%. The R^2 value for the operation-duration prediction model, shown in Figure 9a, is 0.9956, and the R^2 value for the energy-consumption prediction model, shown in Figure 9b, is 0.8689.

$$t(x) = -251657 + 358425(sin(x) + cos(x)) - 100980(sin(2x) + cos(2x)) \tag{25}$$

$$e(x) = -882.495 + 1239.68(sin(x) + cos(x)) - 292.881(sin(2x) + cos(2x)) \tag{26}$$

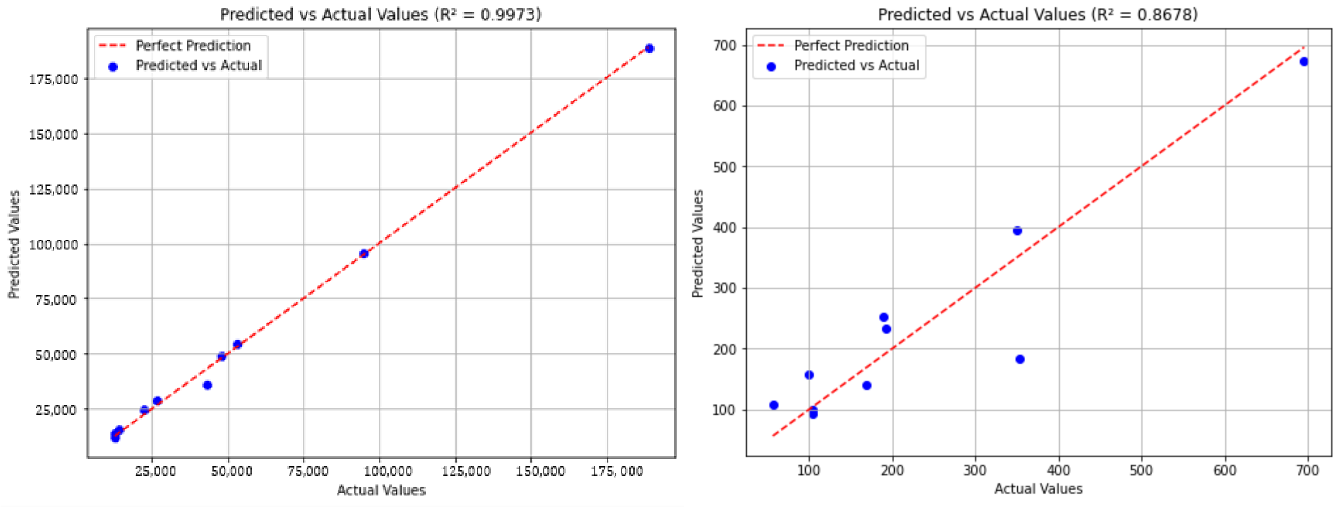

(**a**) (**b**)

Figure 8. (**a**) R^2 graph of operation-duration prediction model. (**b**) R^2 graph of energy-consumption prediction model.

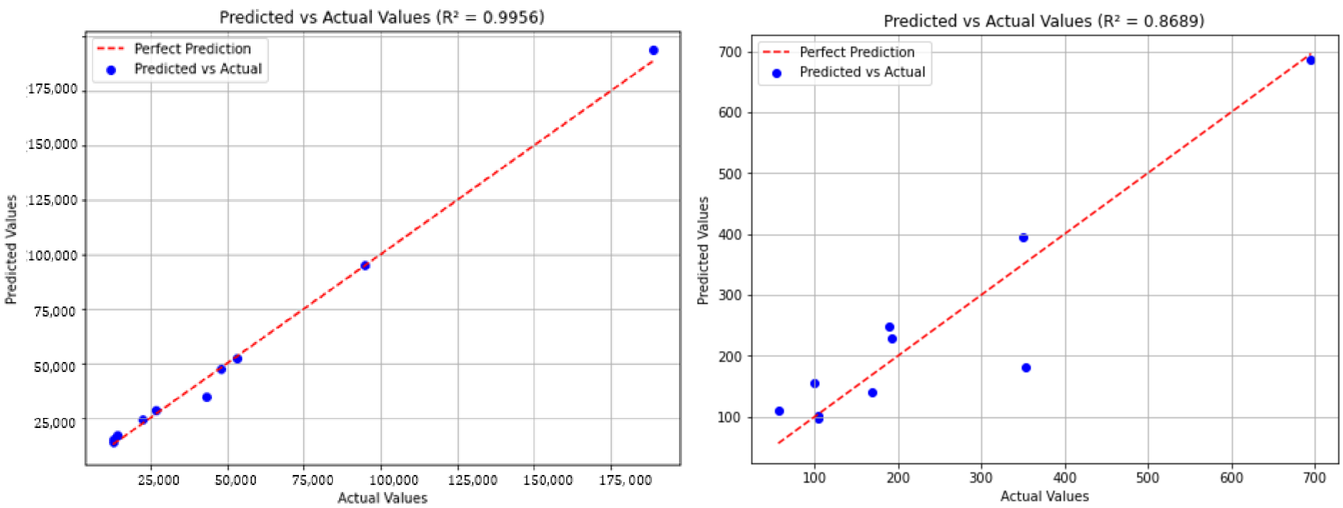

(**a**) (**b**)

Figure 9. (**a**) R^2 graph of operation-duration prediction model. (**b**) R^2 graph of energy-consumption prediction model.

Consequently, when accounting for a variable feed rate, the best estimate using curve fitting resulted in an error of 6.28%. Attempts to model the impact of variation on displacement duration and total power consumption did not yield satisfactory accuracy through curve fitting alone. This indicates that physical parameters such as motion and energy consumption are not fully correlated with the observed duration and total energy usage. Several factors contribute to these discrepancies, including internal resistance changes due to stepper motor temperature, production tolerances of copper wiring within motors, metal expansion in mechanical components, and manufacturing tolerances in electronic systems like CNC boards and transformers. Additionally, the motor control algorithms in CNC boards influence both duration and energy consumption.

4.2. Deep Neural Network Model

To improve predictive performance and ensure broader applicability across different CNC machines, we propose an intelligent hybrid model. This model integrates physical parameters with a data-driven approach. By leveraging AI, the model can infer the influence of unmeasured parameters based on available inputs and outputs, enhancing both the accuracy and generalizability of predictions. Therefore, as shown in Equation (27), the model will provide both time and energy predictions based on the ratio of displacement to feed rate of the CNC machine, the amount of displacement, and the feed rate.

$$[t(x),\ p(x)] = f\left(\frac{m}{v},\ m,\ v\right) \tag{27}$$

To develop a DNN model, four hidden layers were implemented. These layers are designed to capture the correlations between the three input parameters and unmeasured factors affecting the output. Fewer than four hidden layers resulted in reduced performance, while adding more layers showed limited improvement. Therefore, the DNN architecture was optimized with four hidden layers to minimize computation time. The output layer consists of two nodes: one representing operation duration and the other representing power consumption. The best-performing models for both linear and arc/circular motion estimations utilized GELU activation functions. For the operation-duration prediction model, the hidden layers contain 40, 29, 69, and 87 nodes, respectively, and it was trained for 18,287 epochs. Similarly, the power-consumption prediction model has the same number of nodes in its hidden layers, but was trained for 14,000 epochs. The Mean Squared Error (MSE) was employed as the loss function, and the models were trained using the Adam Optimizer with the following hyperparameters: a learning rate of 0.001, beta1 of 0.9, beta2 of 0.999, and epsilon of 1×10^{-7}. Random weights are employed to the nodes at the beginning of the training. The presented models were trained with the specified configuration using the dataset published on IEEE dataport [35]. The dataset was divided into a training set for model development and a test set for performance evaluation, as presented in Table 3.

Table 3. Parameters of training and test datasets.

Training		Test	
Feed Rate (mm/min)	**Motion Amount (cm)**	**Feed Rate (mm/min)**	**Motion Amount (cm)**
125, 250, 500, 750, 1000	10, 25, 50, 75, 100, 115, 135, 150, 175, 200, 215, 235, 250, 300	125, 250, 300, 500, 600, 750, 900, 1000	15, 35, 65, 85, 125, 165, 185, 225, 285

4.3. Hyperparameter Optimization

We employ an iterated local search (ILS) algorithm to find the best solutions for combinations of activation functions, the number of nodes in the hidden layer, and the number of training epochs. During the iterated search phase, the algorithm performs 24 random jumps for the number of nodes in the hidden layer, 10 random jumps for the number of epochs, and 5 random selections of activation functions. After each jump, in the hill-climbing phase, the search algorithm attempts to climb by making at least ten local jumps. During hill climbing, the following activation functions are considered for random selection: Linear, Softplus, Softmax, Tanh, Sigmoid, Swish, ELU, ReLU, and GELU. Specific restrictions are applied throughout the selection process to guide the search towards optimal solutions.

1. Use a “softplus” activation function at the output layer.
2. If the “elu” activation function is assigned to the first and the last hidden layer, an activation function other than “elu” is used for all other layers.
3. If the activation function “elu” is not selected, all nodes will receive the same activation function.

Figure 10 illustrates the change in the objective value throughout the search iterations. As shown, the best solution was not found within the first 300 iterations. However, after increasing the number of nodes in the hidden layers, the algorithm began to identify better solutions. This indicates that the optimal solution can be achieved with a slight increase in the number of nodes from the initial configuration. Moreover, this smaller topology results in lower computational demands, making it more efficient.

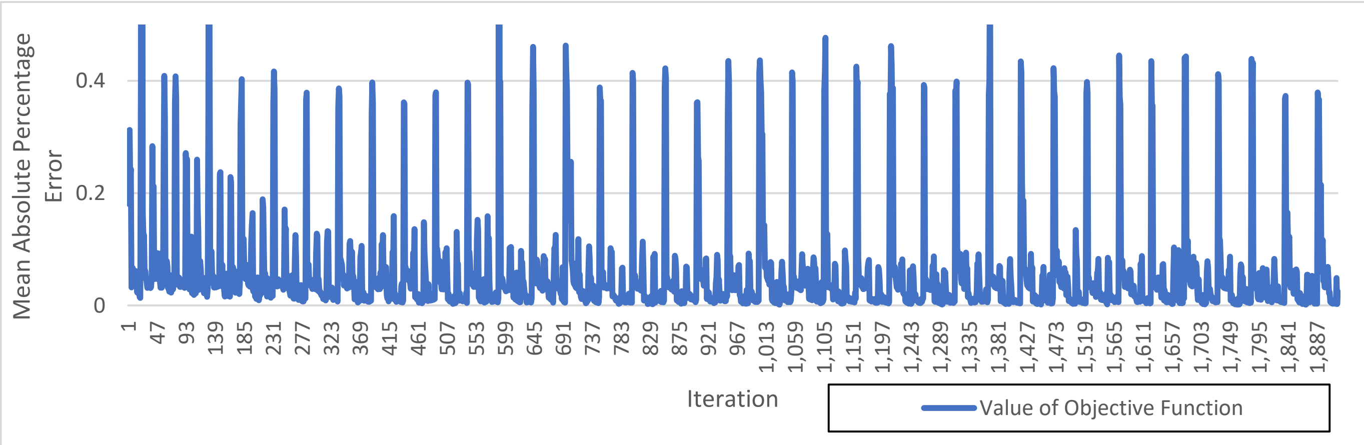

Figure 10. Loss function of the best linear-motion model.

Table 4 presents the top 10 models generated by the ILS algorithm for linear motion-related estimations. The best-performing model features fewer nodes in the hidden layers and a higher number of training epochs compared to the other models, highlighting an effective balance between network complexity and training duration.

Table 4. Performance of the best topologies for linear motion.

Act. Func.	Num of Nodes	Epoch	MAPE of Duration	MAPE of Power Consumption	R^2 of Duration	R^2 of Power Consumption
gelu	40, 29, 69, 87, 2	18,287	0.0057	0.0063	0.9999	0.9999
gelu	86, 51, 80, 132, 2	13,768	0.0071	0.0077	0.9999	0.9999
gelu	65, 38, 80, 97, 2	13,888	0.0073	0.0077	0.9999	0.9999
gelu	86, 39, 80, 132, 2	17,444	0.0078	0.0080	0.9999	0.9998
gelu	86, 39, 80, 132, 2	13,451	0.0081	0.0081	0.9998	0.9998
gelu	60, 31, 80, 87, 2	14,155	0.0082	0.0092	0.9998	0.9997
gelu	78, 39, 80, 132, 2	17,115	0.0088	0.0095	0.9997	0.9997
gelu	65, 39, 80, 114, 2	10,410	0.0090	0.0099	0.9997	0.9997
gelu	86, 39, 80, 132, 2	12,002	0.0091	0.012	0.9997	0.9995
gelu	24, 22, 69, 87, 2	18,842	0.0095	0.015	0.9997	0.9992

The loss function of the best linear-motion model, trained over 18,287 epochs, is shown in Figure 11a. For operation duration, the model achieves a MAPE of 0.0056 and an R^2 of 0.9999, as illustrated in Figure 11b. Regarding energy consumption, the model yields a MAPE of 0.0063 and an R^2 of 0.9999, as shown in Figure 11c.

Table 5 presents the top 10 models generated by the ILS algorithm for arc/circle motion-related estimations. The best-performing model features fewer nodes in the hidden layers and a smaller number of training epochs when compared with linear motion models. It exhibits lower prediction accuracy for energy consumption.

The loss function of the best arc/circle motion model, trained over 14,797 epochs, is shown in Figure 11a. For operation duration, the model achieves a MAPE of 0.0021 and an R^2 of 1, as illustrated in Figure 12b. Regarding energy consumption, the model yields a MAPE of 0.0154 and an R^2 of 0.9992, as shown in Figure 12c.

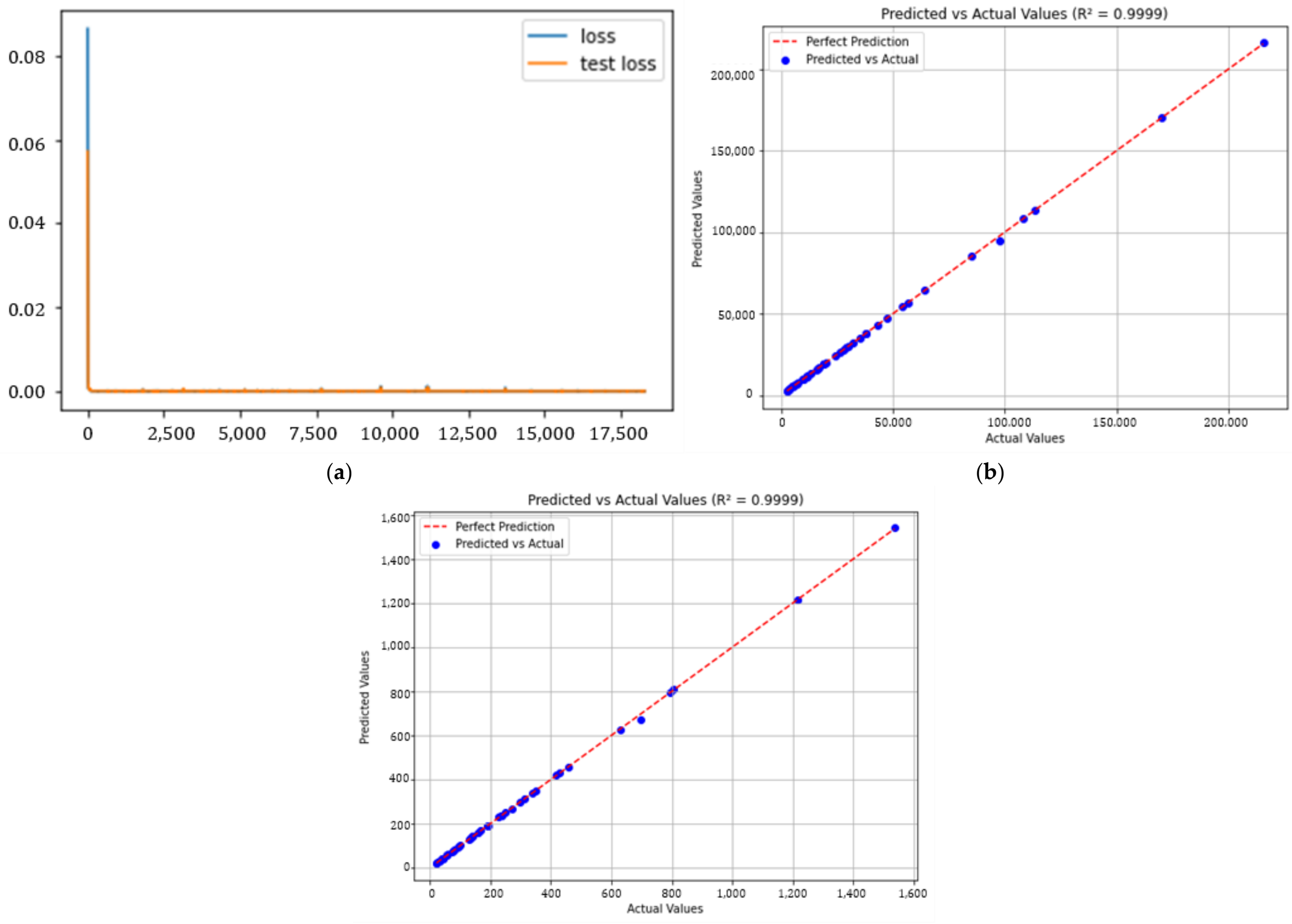

Figure 11. (**a**) Loss function of the best linear-motion model. (**b**) R^2 graph of operation-duration prediction model. (**c**) R^2 graph of energy-consumption prediction model.

Table 5. Performance of the best topologies for arc/circle motion.

Act. Func.	Num of Nodes	Epoch	MAPE of Duration	MAPE of Power Consumption	R^2 of Duration	R^2 of Power Consumption
gelu	40, 29, 69, 87, 2	14,792	0.0021	0.0154	1	0.9992
gelu	105, 51, 80, 132, 2	11,362	0.0025	0.016	1	0.9992
gelu	78, 39, 80, 114, 2	13,348	0.0032	0.0171	1	0.999
gelu	24, 17, 41, 66, 2	15,245	0.0035	0.0175	1	0.9989
gelu	65, 39, 80, 97, 2	11,434	0.0038	0.019	1	0.9987
gelu	65, 31, 80, 97, 2	12,416	0.0045	0.0221	1	0.9986
gelu	60, 31, 80, 87, 2	10,347	0.0046	0.0225	0.9999	0.9985
gelu	40, 29, 69, 87, 2	14,792	0.0049	0.0229	0.9999	0.9984
gelu	24, 17, 69, 87, 2	13,666	0.0052	0.0243	0.9999	0.998
gelu	86, 39, 80, 132, 2	12,376	0.0055	0.0248	0.9999	0.9978

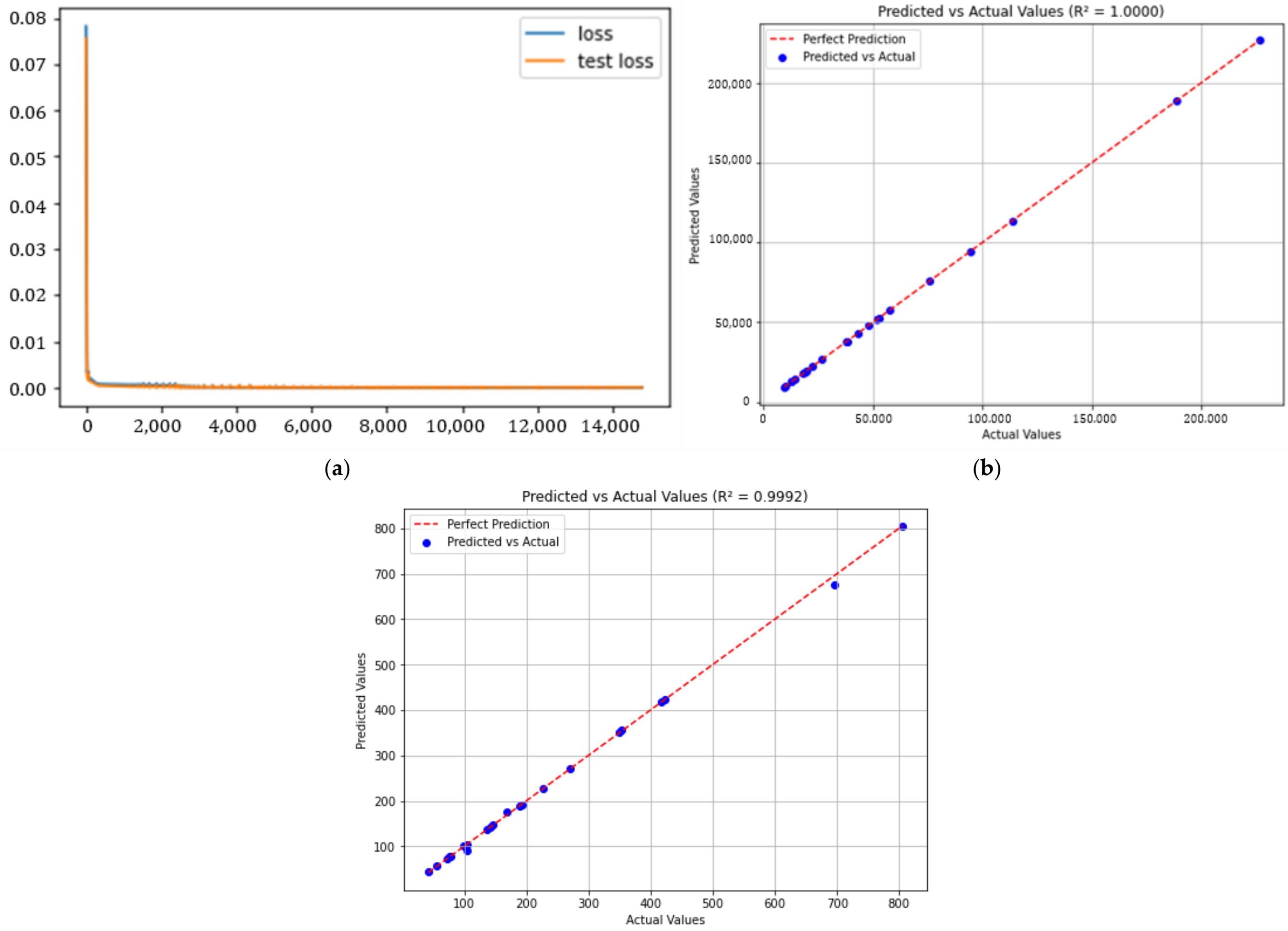

(c)

Figure 12. (**a**) Loss function of the best arc/circle motion model. (**b**) R^2 graph of operation-duration prediction model. (**c**) R^2 graph of energy-consumption prediction model.

4.4. Deep Neural Network Model Without Physical Model Input

To assess the proposed model's efficiency, we removed the physical model input from Equation (28) and built models with the same topology as those optimized by the ILS algorithm. Table 6 shows the performance of these models.

$$[t(x),\ p(x)] = f(m,\ v) \tag{28}$$

Table 6. Performance of the best topologies for linear motion.

Act. Func.	Num of Nodes	Epoch	MAPE of Duration	MAPE of Power Consumption	R^2 of Duration	R^2 of Power Consumption
gelu	40, 29, 69, 87, 2	18,287	0.0058	0.0068	0.9999	0.9999
gelu	65, 38, 80, 97, 2	13,888	0.0079	0.0087	0.9999	0.9998
gelu	86, 51, 80, 132, 2	13,768	0.0083	0.0091	0.9999	0.9998
gelu	60, 31, 80, 87, 2	14,155	0.0088	0.0099	0.9998	0.9998
gelu	24, 22, 69, 87, 2	18,842	0.0092	0.0105	0.9998	0.9997
gelu	86, 39, 80, 132, 2	13,451	0.0096	0.0112	0.9997	0.9997
gelu	86, 39, 80, 132, 2	17,444	0.0098	0.0126	0.9997	0.9996
gelu	78, 39, 80, 132, 2	17,115	0.0114	0.0129	0.9996	0.9995
gelu	86, 39, 80, 132, 2	12,002	0.0119	0.0137	0.9995	0.9993
gelu	65, 39, 80, 114, 2	10,410	0.0122	0.0141	0.9995	0.9993

Figure 13a shows the loss function of the best linear motion model, trained over 18,287 epochs. The model achieves a MAPE of 0.0058 and R^2 of 0.9999 for operation duration in Figure 13b, and a MAPE of 0.0068 with R^2 of 0.9999 for energy consumption in Figure 13c.

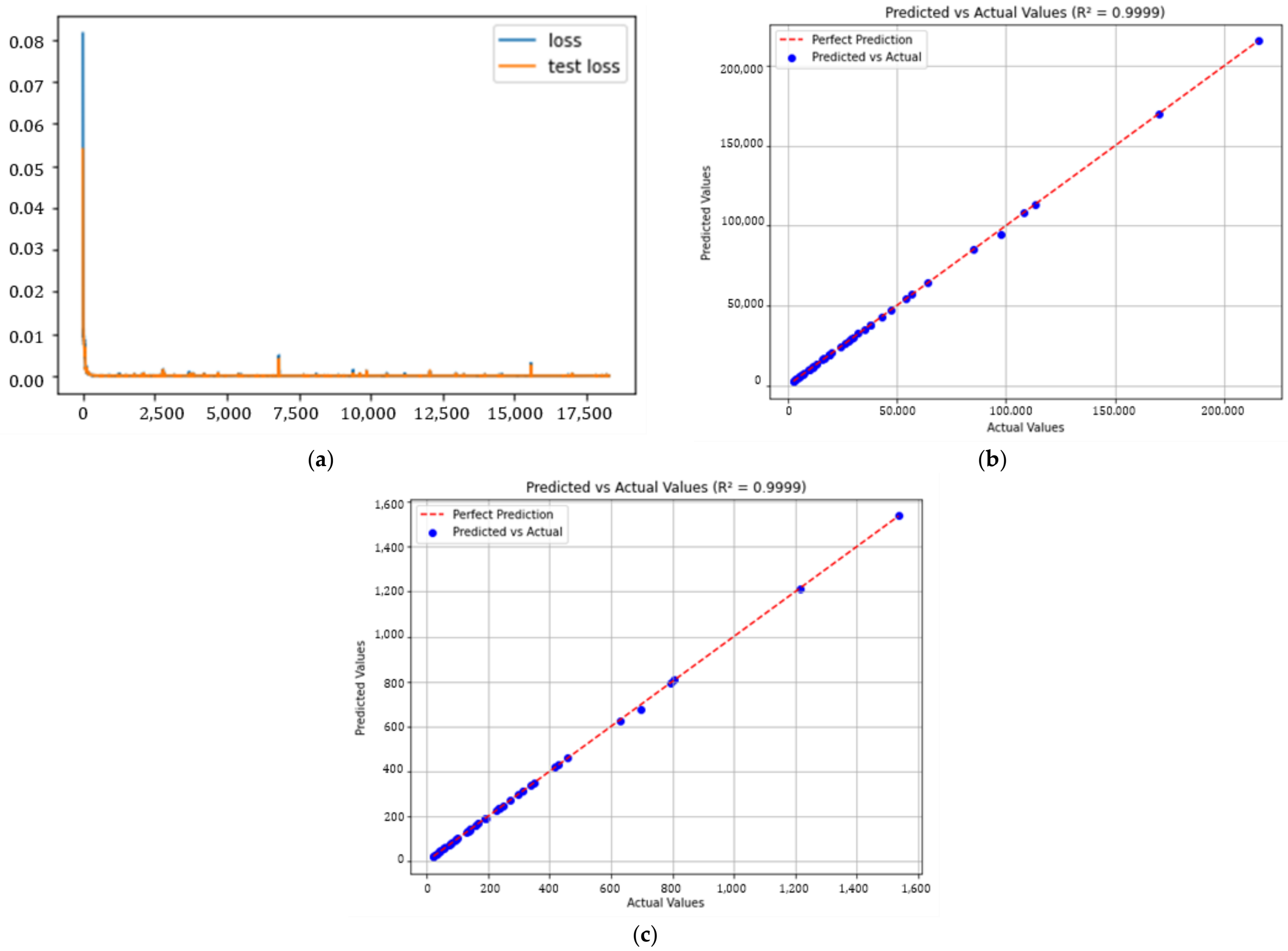

Figure 13. (**a**) Loss function of the best linear motion model. (**b**) R^2 graph of operation-duration prediction model. (**c**) R^2 graph of energy-consumption prediction model.

Table 7 presents the performance of the models in Table 5 which are trained with only measured sensor data.

Table 7. Performance of the best topologies for arc/circle motion.

Act. Func.	Num of Nodes	Epoch	MAPE of Duration	MAPE of Power Consumption	R^2 of Duration	R^2 of Power Consumption
gelu	40, 29, 69, 87, 2	14,792	0.0077	0.0291	0.9999	0.9956
gelu	24, 17, 41, 66, 2	15,245	0.0085	0.032	0.9998	0.9948
gelu	65, 31, 80, 97, 2	12,416	0.0087	0.0354	0.9998	0.9949
gelu	40, 29, 69, 87, 2	14,792	0.0091	0.0362	0.9997	0.9942
gelu	65, 39, 80, 97, 2	11,434	0.0094	0.0371	0.9997	0.9941
gelu	78, 39, 80, 114, 2	13,348	0.0099	0.0376	0.9997	0.9938
gelu	60, 31, 80, 87, 2	10,347	0.0115	0.0397	0.9996	0.9941
gelu	24, 17, 69, 87, 2	13,666	0.0121	0.0413	0.9995	0.9933
gelu	105, 51, 80, 132, 2	11,362	0.0154	0.0479	0.9992	0.9928
gelu	86, 39, 80, 132, 2	12,376	0.0198	0.0523	0.9987	0.992

The loss function of the best arc/circle motion model, trained over 14,797 epochs, is shown in Figure 14a. For operation duration, the model achieves a MAPE of 0.0077 and an R^2 of 0.9999, as illustrated in Figure 14b. Regarding energy consumption, the model yields a MAPE of 0.0291 and an R^2 of 0.9956, as shown in Figure 14c.

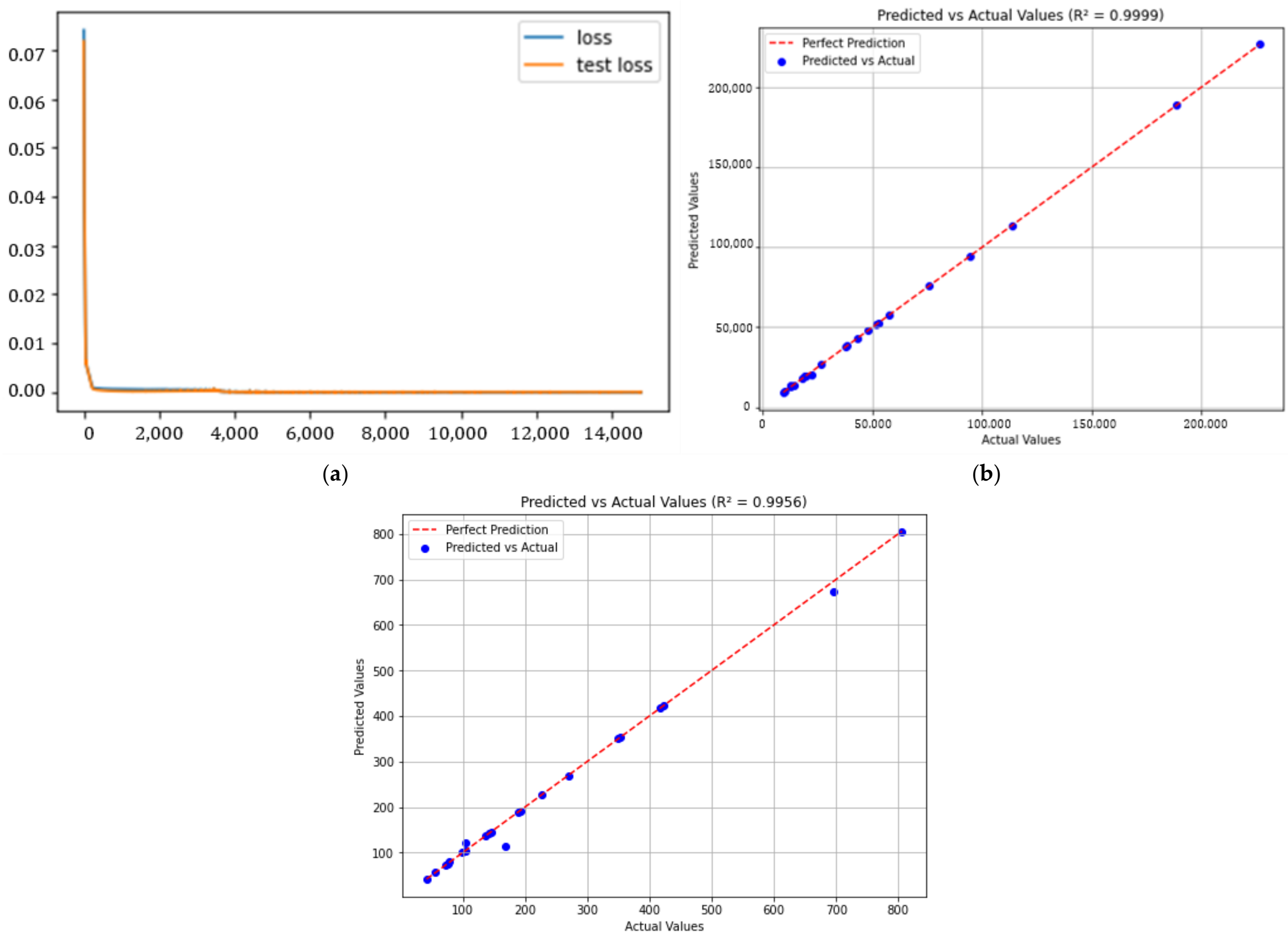

(c)

Figure 14. (**a**) Loss function of the best arc/circle motion model. (**b**) R^2 graph of operation-duration prediction model. (**c**) R^2 graph of energy-consumption prediction model.

When the same models are trained on the same dataset, their performance ranking changes, due to the randomness of initial weights. Since training starts with random weights, generating more models with the same topology can lead to different solutions. Using fixed weights could eliminate this variation, but would hinder hyperparameter optimization by forcing the process to start from the same point, increasing the risk of getting stuck in a local optimum. Our study shows that including the physical model input during training improves AI model performance and reduces prediction variability, as seen by comparing the loss functions in Figures 11a and 13a.

5. Conclusions

Our study presents a comprehensive model with broad industrial applications, focusing on predicting operation time and energy consumption based on G-Code parameters. The novelty of this research lies in correlating G-Code parameters directly with predictions of operation duration and energy consumption, whereas most previous studies rely on derived parameters such as cut depth and cut area, which require calculations from multiple lines of G-Code. In this way, our approach facilitates the optimization of G-Code parameters with respect to energy consumption, while considering operation time constraints. This model can serve as a foundational framework for future research on energy-efficient scheduling. Additionally, our study introduces an AI methodology for modeling the impact of unmeasured factors, such as varying internal resistance and mechanical expansion, on power consumption. By proposing an AI model, we enhance the adaptability of the framework for practical application across various machines and robots.

The proposed model considers machine speed, as variations in speed impact both energy consumption and processing time. Due to the non-linear relationship between these factors, we demonstrated the need for a non-linear model through curve-fitting analysis, making AI the ideal solution for this complexity. A key contribution of our work is the hybrid approach, which combines physical-based formulations with sensor data to improve performance. Another significant contribution is our model's ability to operate on individual G-Code parameters, unlike most studies that rely on multiple G-Codes to derive parameters like cut depth and area. This flexibility allows the model to adapt to various non-linear cut shapes, while others focus mainly on linear geometries. By predicting both operation time and energy consumption for each G-Code line, our model supports optimization in the context of scheduling, bridging the gap between manufacturing engineering and production planning. This integration may be a noteworthy contribution to the literature in these fields, as a future perspective. Additionally, we propose a DNN model suitable for transfer learning, making it adaptable to different machines. Trained under no-load conditions, the model can be fine-tuned for specific factors such as material hardness or machine configurations. It also functions as a pre-trained model for larger DNNs, enabling faster adaptation to new datasets through transfer learning. Our most significant contribution is to the field of sustainability, where we propose a foundational model that can be used for energy-efficient manufacturing and scheduling studies.

In summary, our aim was to develop a precise model that can be adapted to various CNC machines and robots, contributing to the field of sustainability. We began by examining the mathematical complexity of the problem, formulating the motion, and performing a curve-fitting analysis based on this formulation. Through this study, we recognized that the problem is highly complex, influenced by numerous environmental and physical factors. To address this complexity, we proposed a DNN model capable of inferring the effects of unmeasured factors on energy consumption. The model is designed to adapt to a wide range of machines and robots operating under different environmental and physical conditions. Our research demonstrated that incorporating G-Code parameters, alongside calculations derived from a physical equation, allows the DNN model to accurately predict both operation duration and energy consumption. This approach offers a valuable contribution to sustainability, particularly in the areas of manufacturing engineering and scheduling. In future work, we plan to explore efficient transfer learning mechanisms to further adapt our model to different CNC machines and robots across various environmental conditions and material hardness levels. Once we have established an effective adaptation strategy, our next step will be to investigate how to seamlessly integrate manufacturing engineering and scheduling functions to optimize efficiency.

Author Contributions: Conceptualization, S.T. and M.R.C.; methodology, S.T., M.R.C. and E.C.; data curation, M.R.C.; software, M.R.C.; validation, E.C.; visualization, E.C.; writing—original draft preparation, M.R.C. and E.C.; writing—review and editing, S.T. All authors have read and agreed to the published version of the manuscript.

Funding: This research received no external funding.

Data Availability Statement: The data used in this study were uploaded by the authors to https://ieee-dataport.org/documents/cnc-operation-time-dataset on 5 May 2023.

Conflicts of Interest: The authors declare no conflicts of interest.

References

1. European Commission. Industry 5.0. Research and Innovation. Available online: https://research-and-innovation.ec.europa.eu/research-area/industrial-research-and-innovation/industry-50_en (accessed on 19 October 2024).
2. Han, F.; Ren, A.; Liu, J.; Yu, L.; Jia, F.; Hou, H.; Liu, Y. Towards Sustainable Industry: A Comprehensive Review of Energy–Economy–Environment System Analysis and Future Trends. *Sustainability* **2024**, *16*, 5085. [CrossRef]
3. Luo, S.; Zhang, L.; Fan, Y. Energy-efficient scheduling for multi-objective flexible job shops with variable processing speeds by grey wolf optimization. *J. Clean. Prod.* **2019**, *234*, 1365–1384. [CrossRef]
4. Wen, X.; Sun, Y.; Ma, H.L.; Chung, S.H. Green smart manufacturing: Energy-efficient robotic job shop scheduling models. *Int. J. Prod. Res.* **2022**, *61*, 5791–5805. [CrossRef]
5. Wei, Z.; Liao, W.; Zhang, L. Hybrid energy-efficient scheduling measures for flexible job-shop problem with variable machining speeds. *Expert Syst. Appl.* **2022**, *197*, 116785. [CrossRef]
6. Fontes, D.B.M.M.; Homayouni, S.M.; Fernandes, J.C. Energy-efficient job shop scheduling problem with transport resources considering speed adjustable resources. *Int. J. Prod. Res.* **2023**, *62*, 867–890. [CrossRef]
7. Weiss, H.A.; Leuning, N.; Hameyer, K.; Hoffmann, H.; Volk, W. Manufacturing efficient electrical motors with a predictive maintenance approach. *CIRP Ann.* **2019**, *68*, 253–256. [CrossRef]
8. El abdelaoui, F.Z.; Jabri, A.; El Barkany, A. Optimization techniques for energy efficiency in machining processes—A review. *Int. J. Adv. Manuf. Technol.* **2023**, *125*, 2967–3001. [CrossRef]
9. Tang, Y.; Shen, L.; Han, S. Low-Carbon Flexible Job Shop Scheduling Problem Based on Deep Reinforcement Learning. *Sustainability* **2024**, *16*, 4544. [CrossRef]
10. Koulamas, C.; Kyparisis, G.J. Flow shop scheduling with two distinct job due dates. *Comput. Ind. Eng.* **2022**, *163*, 107835. [CrossRef]
11. Ibn-Mohammed, T.; Randall, C.; Mustapha, K.; Guo, J.; Walker, J.; Berbano, S.; Koh, S.; Wang, D.; Sinclair, D.; Reaney, I.; et al. Decarbonising ceramic manufacturing: A techno-economic analysis of energy efficient sintering technologies in the functional materials sector. *J. Eur. Ceram. Soc.* **2019**, *39*, 5213–5235. [CrossRef]
12. Ramesh, J.; Ram, M.M.; Varadarajan, Y.S. Barrier mitigation strategies to the deployment of renewable and energy-efficient technologies (REET) in micro and small manufacturing clusters. *Mater. Today Proc.* **2022**, *52*, 1622–1632. [CrossRef]
13. Hanes, R.; Carpenter, A.; Riddle, M.; Graziano, D.J.; Cresko, J. Quantifying adoption rates and energy savings over time for advanced energy-efficient manufacturing technologies. *J. Clean. Prod.* **2019**, *232*, 925–939. [CrossRef]
14. Oguntola, O.; Boakye, K.; Simske, S. Towards Leveraging Artificial Intelligence for Sustainable Cement Manufacturing: A Systematic Review of AI Applications in Electrical Energy Consumption Optimization. *Sustainability* **2024**, *16*, 4798. [CrossRef]
15. Liu, P.; Zhou, Y.; Zhou, D.K.; Xue, L. Energy Performance Contract models for the diffusion of green-manufacturing technologies in China: A stakeholder analysis from SMEs' perspective. *Energy Policy* **2017**, *106*, 59–67. [CrossRef]
16. Quader, M.A.; Ahmed, S.; Ghazilla, R.A.R.; Ahmed, S.; Dahari, M. A comprehensive review on energy efficient CO_2 breakthrough technologies for sustainable green iron and steel manufacturing. *Renew. Sustain. Energy Rev.* **2015**, *50*, 594–614. [CrossRef]
17. Jahanger, A.; Ozturk, I.; Onwe, J.C.; Joseph, T.E.; Hossain, M.R. Do technology and renewable energy contribute to energy efficiency and carbon neutrality? Evidence from top ten manufacturing countries. *Sustain. Energy Technol. Assess.* **2023**, *56*, 103084. [CrossRef]
18. Zhao, F.; Xu, Z.; Xie, X. Exploring the Role of Digital Economy in Enhanced Green Productivity in China's Manufacturing Sector: Fresh Evidence for Achieving Sustainable Development Goals. *Sustainability* **2024**, *16*, 4314. [CrossRef]
19. Geng, D.; Evans, S.; Kishita, Y. The identification and classification of energy waste for efficient energy supervision in manufacturing factories. *Renew. Sustain. Energy Rev.* **2023**, *182*, 113409. [CrossRef]
20. Hu, L.; Zheng, H.; Shu, L.; Jia, S.; Cai, W.; Xu, K. An investigation into the method of energy monitoring and reduction for machining systems. *J. Manuf. Syst.* **2020**, *57*, 390–399. [CrossRef]
21. Ma, S.; Zhang, Y.; Lv, J.; Ge, Y.; Yang, H.; Li, L. Big data driven predictive production planning for energy-intensive manufacturing industries. *Energy* **2020**, *211*, 118320. [CrossRef]
22. Noor, K.; Siddiqui, M.A.; Syed, A.I. Optimization of specific energy consumption in CNC turning of a hardened alloy steel roll at low cutting speeds. *J. Eng. Des. Technol.* 2023, *ahead-of-print*. [CrossRef]
23. Cai, W.; Liu, F.; Hu, S. An analytical investigation on energy efficiency of high-speed dry-cutting CNC hobbing machines. *Int. J. Sustain. Eng.* **2018**, *11*, 412–419. [CrossRef]
24. Mikhov, M.; Zhilevski, M. Study of Energy Efficiency in a Class of CNC Machine Tools. In Proceedings of the HORA 2021—3rd International Congress on Human-Computer Interaction, Optimization and Robotic Applications, Ankara, Turkey, 11–13 June 2021. [CrossRef]
25. Kozlov, G.; Ivanova, T.; Muyzemnek, A. Improving the energy efficiency of CNC grinding machines. *Univ. Proc. Volga Reg. Tech. Sci.* **2022**, *4*, 171–183. [CrossRef]
26. Shi, J.; Bi, Q.; Wang, Y. Five-axis interpolation of continuous short linear trajectories for 3[PP]S-XY hybrid mechanism by dual Bezier blending. *J. Shanghai Jiaotong Univ. Sci.* **2016**, *21*, 90–102. [CrossRef]
27. Saikumar, N.; Dinesh, N.S.; Kammardi, P. Experience mapping based prediction controller for the smooth trajectory tracking of DC motors. *Int. J. Dyn. Control* **2017**, *5*, 704–720. [CrossRef]

28. Lavernhe, S.; Tournier, C.; Lartigue, C. Kinematical performance prediction in multi-axis machining for process planning optimization. *Int. J. Adv. Manuf. Technol.* **2008**, *37*, 534–544. [CrossRef]
29. Gurgenc, T.; Ucar, F.; Korkmaz, D.; Ozel, C.; Ortac, Y. A study on the extreme learning machine based prediction of machining times of the cycloidal gears in CNC milling machines. *Prod. Eng.* **2019**, *13*, 635–647. [CrossRef]
30. Shin, S.; Woo, J.; Rachuri, S. Energy ef fi ciency of milling machining: Component modeling and online optimization of cutting parameters. *J. Clean. Prod.* **2017**, *161*, 12–29. [CrossRef]
31. Endo, M.; Sencer, B. Accurate prediction of machining cycle times by data-driven modelling of NC system's interpolation dynamics. *CIRP Ann.* **2022**, *71*, 405–408. [CrossRef]
32. Kara, S.; Li, W. Unit process energy consumption models for material removal processes. *CIRP Ann. Manuf. Technol.* **2011**, *60*, 37–40. [CrossRef]
33. Bhinge, R.; Park, J.; Law, K.H.; Dornfeld, D.A.; Helu, M.; Rachuri, S. Toward a Generalized Energy Prediction Model for Machine Tools. *J. Manuf. Sci. Eng. Trans. ASME* **2017**, *139*, 041013. [CrossRef]
34. Skogsrud, S.S.; Winder, W.; Jeon, S. Grbl CNC Controller. Available online: https://github.com/grbl (accessed on 19 October 2024).
35. Cesur, M.R.; Cesur, E. CNC Operation Time Dataset. *IEEE Dataport*. Available online: https://ieee-dataport.org/documents/cnc-operation-time-dataset (accessed on 5 May 2023). [CrossRef]